Aqueous solvation from the water perspective

Saima Ahmed, Andrea Pasti, Ricardo J. Fernández-Terán, Gustavo Ciardi, Andrey Shalit, and Peter Hamm

Citation: The Journal of Chemical Physics **148**, 234505 (2018); doi: 10.1063/1.5034225
View online: https://doi.org/10.1063/1.5034225
View Table of Contents: http://aip.scitation.org/toc/jcp/148/23
Published by the American Institute of Physics

Articles you may be interested in

How proteins modify water dynamics
The Journal of Chemical Physics **148**, 215103 (2018); 10.1063/1.5026861

Perspective: How to understand electronic friction
The Journal of Chemical Physics **148**, 230901 (2018); 10.1063/1.5035412

The spatial range of protein hydration
The Journal of Chemical Physics **148**, 215104 (2018); 10.1063/1.5031005

Communication: Diffusion constant in supercooled water as the Widom line is crossed in no man's land
The Journal of Chemical Physics **148**, 191102 (2018); 10.1063/1.5029822

Time correlation functions of simple liquids: A new insight on the underlying dynamical processes
The Journal of Chemical Physics **148**, 174501 (2018); 10.1063/1.5025120

Preface: Special Topic on Ions in Water
The Journal of Chemical Physics **148**, 222501 (2018); 10.1063/1.5039655

PHYSICS TODAY
WHITEPAPERS

ADVANCED LIGHT CURE ADHESIVES

Take a closer look at what these environmentally friendly adhesive systems can do

READ NOW

PRESENTED BY
MASTERBOND
ADHESIVES | SEALANTS | COATINGS

Aqueous solvation from the water perspective

Saima Ahmed, Andrea Pasti, Ricardo J. Fernández-Terán, Gustavo Ciardi, Andrey Shalit, and Peter Hamm
Department of Chemistry, University of Zurich, Zurich, Switzerland

(Received 10 April 2018; accepted 16 May 2018; published online 19 June 2018)

The response of water re-solvating a charge-transfer dye (deprotonated Coumarin 343) after photoexcitation has been measured by means of transient THz spectroscopy. Two steps of increasing THz absorption are observed, a first ~10 ps step on the time scale of Debye relaxation of bulk water and a much slower step on a 3.9 ns time scale, the latter of which reflecting heating of the bulk solution upon electronic relaxation of the dye molecules from the S_1 back into the S_0 state. As an additional reference experiment, the hydroxyl vibration of water has been excited directly by a short IR pulse, establishing that the THz signal measures an elevated temperature within ~1 ps. This result shows that the first step upon dye excitation (10 ps) is not limited by the response time of the THz signal; it rather reflects the reorientation of water molecules in the solvation layer. The apparent discrepancy between the relatively slow reorientation time and the general notion that water is among the fastest solvents with a solvation time in the sub-picosecond regime is discussed. Furthermore, non-equilibrium molecular dynamics simulations have been performed, revealing a close-to-quantitative agreement with experiment, which allows one to disentangle the contribution of heating to the overall THz response from that of water orientation. *Published by AIP Publishing.* https://doi.org/10.1063/1.5034225

I. INTRODUCTION

Dynamic Stokes shift experiments have been among the first ultrafast experiments in the solution phase and have been pursued on numerous molecular systems whenever corresponding nano-,[1] pico-,[2,3] and eventually femtosecond lasers[4,5] became available. This work culminated in a seminal review article by Maroncelli and co-workers.[6] The common picture of the dynamic Stokes shift is shown in Fig. 1. One starts from a thermalized (Gaussian) ensemble in the electronic ground state S_0 of a dye molecule and vertically promotes it to the electronically excited state S_1 with an ultrashort laser pulse according to the Franck-Condon principle. In the S_1, the ensemble will be in a non-equilibrium situation since the free energy curves are displaced with respect to each other. The ensemble therefore relaxes on the S_1 free energy curve on a time scale that we will denote as solvation time τ_S. The relaxation is typically depicted as a reorientation of solvent molecules in the solvation layer. As the ensemble relaxes, the energy gap between the S_1 and S_0 free energy surfaces decreases, which can be observed experimentally as a time-dependent red-shift of the fluorescence or stimulated emission.

For rigid dye molecules with high fluorescence quantum yield in a polar solvent such as water, the dynamic Stokes shift is dominated by the relaxation of solvation degrees of freedom, rather than by intramolecular degrees of freedom, which is why it does not really matter which particular dye is used as a sensor of the solvent response.[7] Even though these experiments measure the dynamics of the solvent, they do it from a solute perspective. On the contrary, here we set out to measure solvation dynamics from the solvent perspective by transient THz spectroscopy. Both perspectives might actually be very different, which can be seen from the in principle well established, but often overlooked and rather non-intuitive fact that the solvation time τ_S and the Debye relaxation time τ_D may deviate significantly. The Debye relaxation time is related to orientational relaxation in the bulk. In the most simple theoretical approach, assuming a continuum model for solvation, a spherical non-polarizable solute molecule, and a single Debye process of the solvent, the solvation time, which sometimes is also called "longitudinal relaxation time," is predicted to be related to the Debye relaxation time[7–12]

$$\tau_S = \frac{2\epsilon_\infty + 1}{2\epsilon_0 + 1}\tau_D, \tag{1}$$

where ϵ_∞ is the dielectric constant from only the electronic polarizability, while ϵ_0 also includes orientational polarizability. In polar solvents, the latter dominates, i.e., $\epsilon_0 \gg \epsilon_\infty$, and Eq. (1) predicts a large separation of time scales between solvation dynamics τ_S and Debye relaxation τ_D. The origin of this time scale separation lies in the very nonlinear dependence of the reaction field R on the dielectric constant ϵ in Onsager's reaction field model

$$R = \frac{2}{r^3}\frac{\epsilon - 1}{2\epsilon + 2}\mu, \tag{2}$$

where r is the radius of the assumed Onsager sphere and μ is the dipole of the molecule. That is, Eq. (1) can be derived from Eq. (2) by plugging in a frequency dependent dielectric constant of a single Debye process,[8]

$$\epsilon(\omega) = \epsilon_\infty + \frac{\epsilon_0 - \epsilon_\infty}{1 - i\omega\tau_D}. \tag{3}$$

In simple words, the nonlinear dependence in Eq. (2) reflects the saturation of the solvent response due to screening; i.e., if the dielectric constant is very much larger than 1 (like for

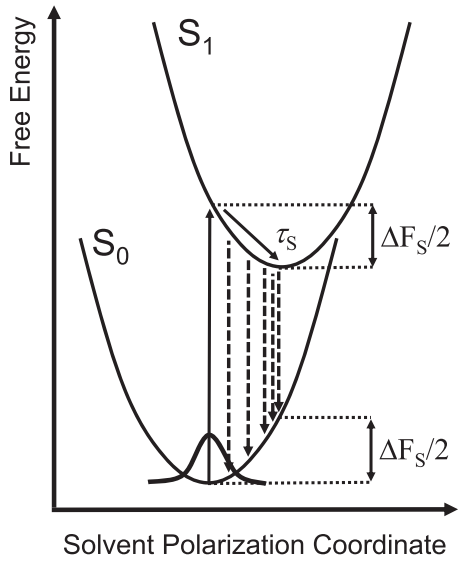

FIG. 1. The textbook picture describing the dynamic Stokes shift of a dye molecule in a polar solvent after electronic excitation. After promoting a thermalized ensemble onto the excited S_1 state, it relaxes with the solvation time τ_S, resulting in a time-dependent red-shift of the fluorescence (dashed arrows).

water), already a thin layer solvates the solute by generating a reaction field R in such a way that the field of the solute's dipole is in essence no longer seen by molecules beyond that layer. If the dielectric constant gets smaller, the size of the solvation layer will get larger, but in such a way that the reaction field will stay almost the same-unless the dielectric constant gets close to 1.

The continuum theory of Eq. (1), obviously, oversimplifies the complexity of the process, which can be seen, for example, from the observed multi-exponential solvation kinetics,[5–7,13] while Eq. (1) would predict a single exponential process. The multi-exponential response has been attributed to many factors, most prominently the failure of the continuum model to account for the discreteness of solvent molecules,[14,15] but also to the fact that the solvent cannot be described by a single Debye process,[16,17] the inertial component of solvation,[9,18] the non-spherical shape of the solute molecule,[16] or translational degrees of freedom that contribute to solvation as well.[9,17,18]

Water is considered to be among the "fastest" solvents with a dominating sub-100 fs inertial component of solvation and a subsequent 800 fs decay, as measured by the dynamic Stokes shift.[5] The solvation dynamics of water have also been measured by a complementary technique, the photon-echo peak shift, revealing three kinetic components (17 fs, 400 fs, and 2.7 ps) and an average solvation time of 400 fs.[13] Given the simplicity of the continuum model, it is remarkable that Eq. (1) predicts a solvation time of 240 fs for water (with $\epsilon_0 \approx 80$, $\epsilon_\infty \approx 1.8$, and $\tau_D = 8.3$ ps[19]), which is quite close to the experimentally observed average solvation time of $\tau_S = 400$ fs (the same semi-quantitative agreement has been found for a wide variety of solvents[6]). From this, one may conclude that the reason for the fast solvation time in water is in fact its large dielectric constant, and not its orientational dynamics *per se*, the latter not being particularly fast with $\tau_D = 8.3$ ps.[19] A recent comprehensive review of the current view of solvation is given in Ref. 7.

To study aqueous solvation from the water perspective, we optically excite a dye molecule and observe the response of the solvent water by transient THz spectroscopy. The THz spectrum of water is related to the dipole-dipole correlation function, whose long-time tail decays exponentially with the Debye relaxation time τ_D. When transiently measuring the THz spectrum of water after exciting a dissolved dye molecule, the expectation is that we observe τ_D rather than τ_S, based on the arguments given above. The present work is in the same spirit as that of Refs. 20 and 21, which, however, studied solvation in organic solvents (probably for reasons of better solubility of the investigated dye molecules), in which case the expected time scale separation according to Eq. (1) is relatively small.

Looking at the problem from a very different angle, the present work is also motivated by the recent observation that solutes, very universally, seem to affect the THz spectrum of a solvation layer that is much larger than commonly assumed (≈10 Å).[22–24] While this interpretation has been strongly challenged, for example by measuring the mobility of individual water molecules with the help of NMR spectroscopy,[25] it has been proposed that the controversy can be resolved by the very delocalized character of THz vibrational modes, which results in correlated motion of many water molecules.[26] If that interpretation is correct, it may be expected that switching the dipole moment of a solute should also affect these delocalized THz modes, resulting in a transient THz signal.

II. METHODS

A. Sample

As sample molecule for this purpose, we chose Coumarin 343, whose solubility in water *per se* is very low (≪ 1 mM). To increase its solubility to 5 mM, we deprotonated, and thereby charged, the dye by the addition of a base (1,4-diazabicyclo[2.2.2]octane, DABCO, 10 mM) to the solution (this base is less nucleophilic than NaOH and thereby prevents degradation of the coumarin due to ring opening). The Stokes shift is 3200 cm^{-1}, as determined from the peaks of the absorption and fluorescence spectra (see Fig. S1 of the supplementary material). The fluorescence quantum yield of a dilute solution of deprotonated Coumarin 343 has been determined to be $\Phi_F = 85\%$ with the help of a Quanta-ϕ integrating sphere calibrated with respect to the reported quantum yield of Coumarin 153 in air-saturated ethanol at room temperature ($\Phi_F = 53\% \pm 4\%$).[27] A fluorescence lifetime of $\tau_F = 4.7$ ns has been measured by time-correlated single photon counting (Horiba Scientific, DeltaDiode DD-395L) in the dilute limit, and we found that it has reduced to $\tau_F = 3.9$ ns at the concentration of the actual THz experiment (5 mM, see Fig. S2 of the supplementary material). We could not reliably measure the quantum yield at these high concentrations due to reabsorption of the emitted light, but we assume that it is reduced by the same factor as the fluorescence lifetime, i.e., $\Phi_F' \approx 70\%$. Finally, we calculated with time-dependent density functional theory at the B3LYP/6-311++G(d,p) level of theory in integral equation formalism polarizable continuum model of water[28] that the

dipole changes by ≈5.3 D when exciting from the ground to the electronically excited state, which agrees well with values reported for the protonated form.[29–31] Note that the absolute dipole moments of the ground and excited states are ill-defined since the molecule is charged; when one chooses the center of nuclear charge as the origin, the dipole increases from 35.2 D in the S_0 to 40.5 D in the S_1 and both are essentially parallel.

B. Transient THz spectroscopy

For the transient THz experiments, we used essentially the same setup as previously described.[32] In brief, pump pulses (400 nm, energy 3.5 μJ) were derived from a 2.5 kHz Ti:S amplifier system (pulse width 120 fs) by frequency doubling in a 0.5 mm thick β-barium borate (BBO) crystal. THz probe pulses were produced by optical rectification in a 0.1 mm thick GaP (110) crystal, generating an almost perfect half-cycle pulse with a FWHM of ≈180 fs (see Fig. S3 of the supplementary material), and detected by electro-optic sampling in a 0.5 mm thick ZnTe (110) crystal, including a recently published concept based on four ZnSe Brewster windows to enhance the detectivity.[33] For a close to diffraction limited imaging of the probe pulses into the sample and into the detection crystal, two computerized numerical control-machined, large-aperture ellipsoidal mirrors have been used. The pump and probe spot sizes in the focus were ≈200 μm. The experimental layout introduces two delay times, the delay t_1 between optical pump-pulse and THz probe pulse and time t_2 that scans the THz pulse. The Coumarin 343/DABCO solution was measured in a 40 μm thick wire-guided water (H_2O) jet[34] to avoid any contamination of the signal from window materials.

As a reference, we also performed an IR-pump-THz-probe experiment, directly exciting the OD band of neat D_2O at 2500 cm^{-1} with 0.7 μJ pulses derived from an IR optical parametric amplifier (OPA).[35] In that case, the sample was held in a cuvette constructed with two 100 μm thin sapphire windows and a spacer of 6 μm. All experiments were performed at room temperature.

Two different pump sources have been used. For experiments with high time resolution, as well as for the IR pump experiment, pump and probe pulses have been derived from the same Ti:S laser system, running the former over an optical delay line. For experiments with long delay times t_1 of up to 50 ns, on the other hand, two Ti:S amplifier systems have been electronically synchronized,[36] revealing an effective time resolution of 10 ps due to the jitter in the synchronization.

C. Simulations

The molecular dynamics (MD) simulation setup is similar to that in Ref. 14 with a large Lennard-Jones sphere solvated in water, thereby mimicking Onsager's solvation model, albeit with a realistic description of the solvent both in terms of its discreteness and dynamics. TIP4P/2005 was used as the water model, whose dielectric constant is $\epsilon_0 = 60$.[37] The Lennard-Jones parameters of the sphere were set to $\epsilon = 0.7794$ kJ/mol and $\sigma = 7.8$ Å, the former being the same as for TIP4P/2005 water and the latter resulting in a sphere radius of 3.9 Å, when considering the corresponding value of TIP4P/2005 (3.2 Å) and the usual combination rule. The sphere was placed in the center of a cubic box of size 25 Å and solvated with 505 water molecules at roughly the experimental density of water. The dipole of the Lennard-Jones sphere was approximated by two point charges separated by 0.8 Å, and the orientation of the dipole was kept fixed during the simulation by restraining these points with harmonic springs. Lennard-Jones interactions were smoothly switched to zero between 10.6 Å and 11.7 Å, and the Coulomb interactions were modelled with the reaction field ($r_c = 10.7$ Å, $\epsilon = \infty$). A time step of 2.5 fs was chosen. The simulation box was equilibrated at 295 K in a 100 ps NVT simulation, thermostated by velocity-rescaling with a coupling constant of 0.5 ps. All simulations were performed with Gromacs.[38]

In order to calculate the non-equilibrium dipole-dipole correlation function of Eq. (4), the following simulation protocol was subsequently used: A 1 ps NVT simulation, introduced to stabilize the temperature, was followed by a 1 ps NVE simulation. From that point on, two 21 ps NVE trajectories were run in parallel: an equilibrium trajectory with the dipole of the Lennard-Jones sphere unchanged and a non-equilibrium trajectory with the dipole changed. In order to accumulate statistics, this protocol was cycled many times (ca. 600 000), continuing from the 21 ps NVE equilibrium trajectory. The simulation parameters were optimized for energy stability during the NVE simulations in order to ensure that the observed temperature change [see Fig. 3(b)] reflects the solvation of the switched dipole, and not any energy drift.

The transient THz response has been calculated from the non-equilibrium dipole-dipole correlation function

$$c(t_1, t_2) = \Delta\langle\dot{\mu}(t_1)\mu(t_1 + t_2)\rangle, \tag{4}$$

where Δ denotes the difference between the non-equilibrium and equilibrium trajectories, t_1 is the pump-probe delay time after switching the dipole of the Lennard-Jones sphere, and t_2 is the time for the THz free induction decay. Time t_1 was evaluated up to 20 ps (of which only 15 ps is shown in Fig. 3) and t_2 up to 1 ps. The dipole $\mu(t)$ contained the contribution of both the Lennard-Jones sphere and all water molecules in the simulation box. This correlation function was subsequently convoluted with the laser pulses to reveal the 3rd-order polarization

$$P^{(3)}(t_1, t_2) = \int_0^\infty \int_0^\infty dt' dt'' E_{THz}(t_2 - t'') \cdot I_{pu}(t_2 + t_1 - t'' - t')c(t', t''), \tag{5}$$

where a Gaussian was assumed for the pump pulse I_{pu} and the second derivative of a Gaussian for the THz pulse E_{THz} (in both cases with a width that matches the experimental pulses). Finally, a time-derivative with respect to t_2 was taken in order to model the emitted 3rd-order THz field,[32]

$$E^{(3)}(t_1, t_2) = \frac{d}{dt_2} P^{(3)}(t_1, t_2). \tag{6}$$

III. RESULTS AND DISCUSSION

Figure 2 (blue) shows the transient THz signal after photoexcitation of the dye molecule, measured at the peak of

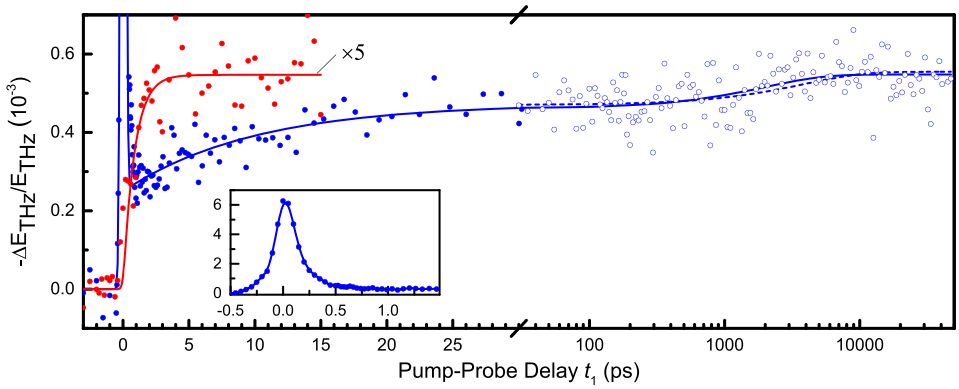

FIG. 2. Relative change of the transmitted THz field E_{THz} measured at the peak of the half-cycle THz pulse. Shown is the response after photoexcitation of Coumarin 343 in water at 400 nm (blue data) or after pumping the hydroxyl vibration of water (D_2O) directly with an IR pulse (red data, smoothed with a 5-point quadratic Savitzky–Golay filter and scaled up by a factor of 5 to match the late time temperature jump in the blue data). The blue filled circles show the data measured with a high time resolution of up to 30 ps plotted on a linear scale, and the blue open circles show those measured with two synchronized laser systems from 30 ps up to 50 ns plotted on a logarithmic scale (both data sets were stitched together by slightly scaling the second one). The solid lines show exponential fits, leaving all time constants as free fit parameters, while the fit shown as the dashed blue line fixes the slowest time constant to 3.9 ns, as determined from the fluorescence decay (see Fig. S2 of the supplementary material). The inset shows the spike around delay zero.

the half-cycle THz pulse ($t_2 = 0$). Two data sets are stitched together in this plot, obtained with the two different pump sources described in Sec. II, thereby covering the time range from 100 fs to 50 ns. Around delay zero, a pulse-width-limited spike of increased THz absorption is observed (see Fig. 2, inset). The spike does not decay to zero completely, but leaves a small pedestal, which is hardly seen in the inset of Fig. 2 and which is what the main panel of Fig. 2 focuses on. This pedestal increases in two steps. The first step, occurring with a time constant of 10 ± 3 ps, agrees within error with the Debye relaxation time of water,[19] while the second step can be fit to a process with 1.9 ns (Fig. 2, solid blue line). The signal stays constant from there on.

It can be safely assumed that water fully thermalizes on a nanosecond time scale over distances, which exceed that between neighboring dye molecules,[39] and we attribute the final pedestal after the second step to the heating of the sample. Indeed, it is known from stationary spectroscopy that the THz absorption cross section of water increases as a function of temperature.[40] To calibrate the effect for our concrete experimental conditions, we measured the transmission of the THz pulse through a thermostated water cuvette of equal thickness at various temperatures and observed a linear dependence with a slope $\Delta T/T = -7.5 \cdot 10^{-3}$ K^{-1} (see Fig. S3 of the supplementary material). With that, one can estimate a total temperature jump of ≈0.07 K from the size of the late-time pedestal of the transient THz data (Fig. 2). This number agrees very well with an independent estimate (0.06 K) obtained from the number of absorbed photons per sample volume, their energy, the heat capacity of water, and the fluorescence quantum yield of the dye.

Based on this discussion, we conclude that the second step observed in the transient THz response reflects heating of the bulk solution upon electronic relaxation of the dye molecule from the S_1 state back into the S_0 state. Since the fluorescence quantum of the dye yield is not 100% (we determined a quantum yield of $\Phi_F = 70\%$; see Sec. II), the remaining fraction of dye molecules dissipates their electronic excitation energy into the solvent upon radiationless relaxation, thereby heating the solvent. The fluorescence lifetime, which can be measured much more accurately (3.9 ns; see Fig. S2 of the supplementary material) deviates from the value obtained from the fit of the transient THz data (1.9 ns). We therefore also show in Fig. 2 a fit that fixes the time constant of that process to 3.9 ns (blue dashed line), evidencing that this is still consistent with the relatively poor signal-to-noise ratio of the transient THz data.

In light of the Introduction, we consider the first step, occurring with a time constant that agrees well with the Debye relaxation time of water, the most important result of this study. Before we continue with its discussion, we need to establish the time scale on which the THz absorption responds to an elevated temperature. To this end, we also performed an IR-pump-THz-probe experiment, in which the hydroxyl vibration of water (D_2O) is excited directly (Fig. 2, red data). It is well established from IR-pump-IR-probe as well as from 2D IR experiments that the lifetime of that vibration is ultrafast, in particular, in isotope-pure D_2O as well as H_2O, and that energy thermalizes on a ∼1 ps time scale.[41–48] And, indeed, the THz-absorption rises very quickly with the fit revealing a time constant of 1 ± 0.3 ps (a complementary experiment, THz-pump-IR-probe, highlighting the coherence in the coupling between inter- and intramolecular modes on subpicosecond time scales, has recently been performed by Bonn and co-workers[49]). Experimental[40] and simulation data (Fig. S4 of the supplementary material) show that the THz absorption increases with temperature throughout the whole frequency range from 0 to 600 cm^{-1}, resulting from a red shift of the librational mode at 600 cm^{-1}. Its low-frequency wing extends into the 100 cm^{-1} regime, where the THz pulses peak, indicating that the mode is almost critically damped. This also explains why the librational mode can respond to an elevated temperature so quickly since a close-to-critical damping is the situation with the fastest possible relaxation. We conclude that the observation of a 10 ps time scale for the first step after photo-excitation of the coumarin dye is not limited by the response time of the THz signal, but rather evidences that the solvent response indeed occurs on that slower time scale.

To get deeper insights into this process, we performed non-equilibrium MD simulations, considering a large Lennard-Jones sphere as solute in water (see Sec. II for details). Figure 3 (blue) shows the result when first equilibrating the system with the dipole of the Lennard-Jones sphere set to zero and then instantaneously switching it on to 7.5 D at $t_1 = 0$, while the red data show the results for the opposite process switching from 7.5 D to 0. When switching the dipole on, the reaction field shown in Fig. 3(a) (blue) can be fit to three exponentials with 7 fs (37%), 210 fs (31%), and 1.6 ps (32%) and an average relaxation time of 590 fs. When switching off the dipole [Fig. 3(a), red], the response is a bit faster with 8 fs (42%), 150 fs (34%), and 1.1 ps (23%) and an average decay time of 310 fs. The slightly different time scale indicates that the system is not quite in a linear response regime, yet, in either case, the result is in very good agreement with the experimental solvation time (400 fs),[13] despite the crudeness of the model.

Figure 3(b) shows the "non-equilibrium temperature" after switching, as determined from the total kinetic energy of the simulation box. When the dipole is switched on (blue), we observe an instantaneous temperature jump followed by a partial decay that can be fit to a single-exponential function with a time constant of 2.2 ps. On the other hand, when switching off the dipole (red), approximately the same initial temperature jump is observed, but the temperature subsequently increases further with a time constant of 3.6 ps. The total amount of dissipated energy upon solvation of the dipole, as measured by the late-time temperature change, is different from that upon re-solvation of the Lennard-Jones sphere without any dipole. Based on Fig. 1, these results might seem surprising. That is, solvation and re-solvation are the equivalents of what would happen on the S_1 electronic state upon electronic excitation and subsequently on the S_0 after emission of a fluorescence photon. Figure 1 would suggest that both events release approximately the same amount of free energy (which is a result of the linear response assumption that renders the curvatures of the S_0 and S_1 free energy surfaces identical). To understand this discrepancy, one must keep in mind that Fig. 1 plots "free energy," while temperature measures "energy." Since solvation is entropy-driven to a significant extent, both terms may be very different. For example, it is a freshman chemistry experiment to observe that dissolution of NaCl in water is endothermic [e.g., temperature may indeed decrease upon solvation, as shown in Fig. 3(b), blue]. Nevertheless, entropy is a function only of the "solvent polarization coordinate" shown in Fig. 1; hence, free energy differences at a given position of that coordinate are in fact the same as energy differences.[9] This is why the dashed arrows in Fig. 1 indeed indicate the energy of the emitted fluorescence photons. Also the total solvation free energy ΔF_S is the same as the Stokes shift ΔE_S. However, while the total solvation free energy splits half/half for the solvation of the excited state and the re-solvation of the ground state, the same is not necessarily true for the splitting of the total solvation energy.

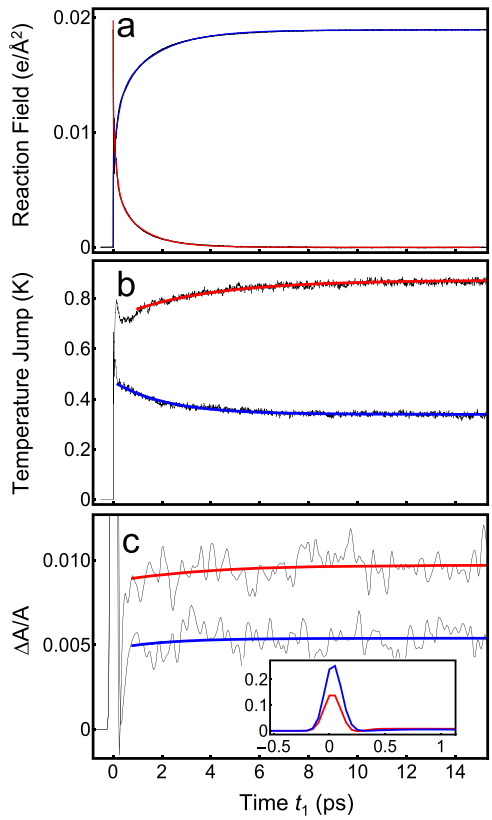

FIG. 3. Simulation results. Panel (a) shows the reaction field $R(t)$ when switching the dipole of the Lennard-Jones sphere on (blue) or off (red), panel (b) shows the solvent temperature in response to the switching (same color code), and panel (c) shows the simulated THz signal in units of relative absorbance change $\Delta A/A$. In either case, the thin black lines present data and the colored lines present single exponential fits. The inset in panel (c) shows the spike around time t_1 zero.

Finally, Fig. 3(c) shows the transient THz response for both switching events, i.e., the result of Eq. (6) along t_1 at the peak of the signal with $t_2 = -50$ fs (the full 2D data set is shown in Fig. S5 of the supplementary material). Around delay zero ($t_1 = 0$), a pulse-width limited spike is observed, just like in experiment [insets of Figs. 3(c) and 2], which represents the electronic contribution from the instantaneous switching of the dipole of the Lennard-Jones sphere. This can be verified by removing its contribution to $\mu(t)$ in Eq. (4), in which case that spike is inverted (and smaller). After the spike, a small pedestal of increased absorbance remains [Fig. 3(c), main panel], which slightly increases further as a function of time in either case [the fit in Fig. 3(c) fixes the time constants to the values obtained from Fig. 3(b) since the data are too noisy and the effect is too small to extract the time scale independently]. While that second step in the simulation results is faster than the Debye relaxation (which is 14 ps for the current simulation setup; see Fig. S6 of the supplementary material), it is still slower than the solvation response [310 fs or 590 fs, see Fig. 3(a)].

Even though Figs. 3(b) and 3(c) resemble each other to a certain extent, evidencing that the THz response can indeed be considered an ultrafast thermometer, they do not do so in all aspects. First, trivially, the initial spike in the THz response is hardly present in the temperature data, as it originates directly from the THz field emitted upon switching the dipole of the Lennard-Jones sphere. Second, while the temperature decreases again after the initial jump when switching on the dipole [Fig. 3(b), blue], the THz absorption continues

to increase [Fig. 3(c), blue]. Third, while the ratio of final temperatures is 2.6 after switching off the dipole [Fig. 3(b), red] *versus* switching it on [Fig. 3(b), blue], the corresponding factor is only 1.8 for the THz response [Fig. 3(c), red, *versus* Fig. 3(c), blue]. Points two and three emphasize that a sizable contribution to the THz response, which reflects the different structuring of water around solutes with different dipoles, exists as well. This is expected since it has been shown that certain solutes affect the THz absorption of solvating water.[22–24,50] For the case when the dipole is switched on, the kinetic response from water orientation actually overcompensates that of the temperature effect. Water reorients on the time scale of Debye relaxation; hence, it appears meaningful that we see that time scale in the THz response. We have no evidence, however, that the orientational response has a different spectral dependence than the temperature response, which would show up as a variation of the t_2-dependence of the THz signal as a function of t_1 (see full 2D data in Fig. S5 of the supplementary material).

With the dipole switched off, the Lennard-Jones sphere is a very hydrophobic particle. Even in that most simple case, the solvation energy and solvation entropy are complicated and not necessarily intuitive functions of parameters such as sphere radius[51] or temperature,[52,53] and one might expect that the situation is even more involved for a real molecule with a complex charge distribution. Anyhow, the simulation of Fig. 3(c) is in very good agreement with the experimental results of Fig. 2, regardless of whether the solute turns into more polar or more apolar upon switching, suggesting that these results are rather universal.

IV. CONCLUSION

In conclusion, we have measured aqueous solvation from a water perspective by means of transient THz spectroscopy. We consider the 10 ps time scale observed for the first step a rather slow process for water. It compares well with the Debye relaxation time, which is the slowest established time scale known for water, suggesting that there is a connection between the two processes. We have also shown that the THz response, for the most part, can be interpreted as an ultrafast thermometer with a response time of ∼1 ps, but the restructured water around the solute contributes as well to a smaller extent. While the sub-picosecond solvation of the excited state of the coumarin dye must imply a partial rearrangement of water molecules in the solvation layer, the time scale separation implies that this happens in a way that strain is built up within the solvation layer. Releasing that strain, apparently, requires an essentially complete reorientation of some of the water molecules in the solvation layer, which is why the Debye relaxation time is the relevant time scale. We consider this experiment to be a direct observation of the very non-intuitive time scale separation between solvation time and Debye relaxation [Eq. (1)].

SUPPLEMENTARY MATERIAL

See supplementary material for absorption and fluorescence spectra of the dye (Fig. S1), a measurement of the excited state lifetime (Fig. S2), the THz pulse after transmitting through a thermalized 40 μm water cuvette as a function of temperature (Fig. S3), simulated absorption spectra of TIP4P/2005 water (Fig. S4), the full simulated THz response as a function of both time coordinates t_1 and t_2 (Fig. S5), and the dipole-dipole correlation function of the simulation box (Fig. S6).

ACKNOWLEDGMENTS

The work has been supported by the Swiss National Science Foundation (SNF) through the NCCR MUST as well as Grant No. 200021_165789/1.

[1] T. Azumi, K.-I. Itoh, and I. Hiroshi, J. Chem. Phys. **65**, 2550 (1976).
[2] L. A. Haliidy and M. R. Topp, J. Phys. Chem. **82**, 2415 (1978).
[3] T. Okamura, M. Sumitani, and K. Yoshihara, Chem. Phys. Lett. **94**, 339 (1983).
[4] W. Jarzeba, G. C. Walker, A. E. Johnson, M. A. Kahlow, and P. F. Barbara, J. Phys. Chem. **92**, 7039 (1988).
[5] R. Jimenez, G. R. Fleming, P. V. Kumar, and M. Maroncelli, Nature **369**, 471 (1994).
[6] M. L. Horng, J. A. Gardecki, A. Papazyan, and M. Maroncelli, J. Phys. Chem. **99**, 17311 (1995).
[7] B. Bagchi and B. Jana, Chem. Soc. Rev. **39**, 1936 (2010).
[8] B. Bagchi, D. W. Oxtoby, and G. R. Fleming, Chem. Phys. **86**, 257 (1984).
[9] G. Van der Zwan and J. T. Hynes, J. Phys. Chem. **89**, 4181 (1985).
[10] R. F. Loring and S. Mukamel, J. Chem. Phys. **87**, 1272 (1986).
[11] D. Kivelson and H. Friedman, J. Phys. Chem. **93**, 7026 (1989).
[12] V. I. Arkhipov and N. Agmon, Isr. J. Chem. **43**, 363 (2003).
[13] M. J. Lang, X. J. Jordanides, X. Song, and G. R. Fleming, J. Chem. Phys. **110**, 5884 (1999).
[14] M. Maroncelli and G. R. Fleming, J. Chem. Phys. **89**, 5044 (1988).
[15] M. Maroncelli, J. Chem. Phys. **94**, 2084 (1991).
[16] B. Bagchi, E. W. Castner, and G. R. Fleming, J. Mol. Struct. **194**, 171 (1989).
[17] L. E. Fried and S. Mukamel, J. Chem. Phys. **93**, 932 (1990).
[18] A. Chandra and B. Bagchi, J. Chem. Phys. **94**, 3177 (1991).
[19] T. Fukasawa, T. Sato, J. Watanabe, Y. Hama, W. Kunz, and R. Buchner, Phys. Rev. Lett. **95**, 197802 (2005).
[20] G. Haran, W. D. Sun, K. Wynne, and R. M. Hochstrasser, Chem. Phys. Lett. **274**, 365 (1997).
[21] R. McElroy and K. Wynne, Phys. Rev. Lett. **79**, 3078 (1997).
[22] S. Ebbinghaus, S. J. Kim, M. Heyden, X. Yu, U. Heugen, M. Gruebele, D. M. Leitner, and M. Havenith, Proc. Natl. Acad. Sci. U. S. A. **104**, 20749 (2007).
[23] M. Heyden, E. Bründermann, U. Heugen, G. Niehues, D. M. Leitner, and M. Havenith, J. Am. Chem. Soc. **130**, 5773 (2008).
[24] K. Meister, S. Ebbinghaus, Y. Xu, J. G. Duman, A. DeVries, M. Gruebele, D. M. Leitner, and M. Havenith, Proc. Natl. Acad. Sci. U. S. A. **110**, 1617 (2013).
[25] L. R. Winther, J. Qvist, and B. Halle, J. Phys. Chem. B **116**, 9196 (2012).
[26] M. Heyden, J. Chem. Phys. **141**, 22D509 (2014).
[27] C. Würth, M. Grabolle, J. Pauli, M. Spieles, and U. Resch-Genger, Nat. Protoc. **8**, 1535 (2013).
[28] M. J. Frisch, G. W. Trucks, H. B. Schlegel, G. E. Scuseria, M. A. Robb, J. R. Cheeseman, G. Scalmani, V. Barone, B. Mennucci, G. A. Petersson, H. Nakatsuji, M. Caricato, X. Li, H. P. Hratchian, A. F. Izmaylov, J. Bloino, G. Zheng, J. L. Sonnenberg, M. Hada, M. Ehara, K. Toyota, R. Fukuda, J. Hasegawa, M. Ishida, T. Nakajima, Y. Honda, O. Kitao, H. Nakai, T. Vreven, J. A. Montgomery, Jr., J. E. Peralta, F. Ogliaro, M. Bearpark, J. J. Heyd, E. Brothers, K. N. Kudin, V. N. Staroverov, R. Kobayashi, J. Normand, K. Raghavachari, A. Rendell, J. C. Burant, S. S. Iyengar, J. Tomasi, M. Cossi, N. Rega, J. M. Millam, M. Klene, J. E. Knox, J. B. Cross, V. Bakken, C. Adamo, J. Jaramillo, R. Gomperts, R. E. Stratmann, O. Yazyev, A. J. Austin, R. Cammi, C. Pomelli, J. W. Ochterski, R. L. Martin, K. Morokuma, V. G. Zakrzewski, G. A. Voth, P. Salvador, J. J. Dannenberg, S. Dapprich, A. D. Daniels, O. Farkas, J. B. Foresman, J. V. Ortiz, J. Cioslowski, and D. J. Fox, GAUSSIAN 09, Revision B.01, Gaussian, Inc., Wallingford, CT, 2009.
[29] N. Nemkovich, H. Reis, and W. Baumann, J. Lumin. **71**, 255 (1997).

[30]R. J. Cave and E. W. Castner, J. Phys. Chem. A **106**, 12117 (2002).
[31]R. Kanya and Y. Ohshima, Chem. Phys. Lett. **370**, 211 (2003).
[32]J. Savolainen, S. Ahmed, and P. Hamm, Proc. Natl. Acad. Sci. U. S. A. **110**, 20402 (2013).
[33]S. Ahmed, J. Savolainen, and P. Hamm, Rev. Sci. Instrum. **85**, 013114 (2014).
[34]M. J. Tauber, R. A. Mathies, X. Chen, and S. E. Bradforth, Rev. Sci. Instrum. **74**, 4958 (2003).
[35]P. Hamm, R. A. Kaindl, and J. Stenger, Opt. Lett. **25**, 1798 (2000).
[36]J. Bredenbeck, J. Helbing, and P. Hamm, Rev. Sci. Instrum. **75**, 4462 (2004).
[37]J. L. Abascal and C. Vega, J. Chem. Phys. **123**, 234505 (2005).
[38]D. Van Der Spoel, E. Lindahl, B. Hess, G. Groenhof, A. E. Mark, and H. J. C. Berendsen, J. Comput. Chem. **26**, 1701 (2005).
[39]T. Lian, B. Locke, Y. Kholodenko, and R. M. Hochstrasser, J. Phys. Chem. **98**, 11648 (1994).
[40]H. R. Zelsmann, J. Mol. Struct. **350**, 95 (1995).
[41]A. J. Lock, S. Woutersen, and H. J. Bakker, J. Phys. Chem. A **105**, 1238 (2001).
[42]A. J. Lock and H. J. Bakker, J. Chem. Phys. **117**, 1708 (2002).
[43]A. Pakoulev, Z. Wang, and D. D. Dlott, Chem. Phys. Lett. **371**, 594 (2003).
[44]T. Steinel, J. B. Asbury, J. Zheng, and M. D. Fayer, J. Phys. Chem. A **108**, 10957 (2004).
[45]M. L. Cowan, B. D. Bruner, N. Huse, J. R. Dwyer, B. Chugh, E. T. J. Nibbering, T. Elsaesser, and R. J. D. Miller, Nature **434**, 199 (2005).
[46]L. Piatkowski, K. B. Eisenthal, and H. J. Bakker, Phys. Chem. Chem. Phys. **11**, 9033 (2009).
[47]J. Lindner, P. Vöhringer, M. S. Pshenichnikov, D. Cringus, D. A. Wiersma, and M. Mostovoy, Chem. Phys. Lett. **421**, 329 (2006).
[48]S. T. Van Der Post, C. S. Hsieh, M. Okuno, Y. Nagata, H. J. Bakker, M. Bonn, and J. Hunger, Nat. Commun. **6**, 8384 (2015).
[49]M. Grechko, T. Hasegawa, F. D'Angelo, H. Ito, D. Turchinovich, Y. Nagata, and M. Bonn, Nat. Commun. **9**, 885 (2018).
[50]D. A. Schmidt, S. Funkner, B. P. Born, R. Gnanasekaran, G. W. Schwaab, D. M. Leitner, and M. Havenith, J. Am. Chem. Soc. **131**, 18512 (2009).
[51]D. Chandler, Nature **437**, 640 (2005).
[52]N. T. Southall, K. A. Dill, and A. D. J. Haymet, J. Phys. Chem. **106**, 521 (2002).
[53]K. A. Dill and T. M. Truskett, Annu. Rev. Biophys. Biomol. Struct. **34**, 173 (2005).